Ferroelectric, piezoelectric, and leakage current properties of $(K_{0.48}Na_{0.48}Li_{0.04})(Nb_{0.775}Ta_{0.225})O_3$ thin films grown by pulsed laser deposition

D. Y. Wang,[1,2,a)] D. M. Lin,[2,a)] K. W. Kwok,[2] N. Y. Chan,[2] J. Y. Dai,[2] S. Li,[1] and H. L. W. Chan[2]

[1]*School of Materials Science and Engineering, The University of New South Wales, Sydney, New South Wales 2052, Australia*

[2]*Department of Applied Physics and Materials Research Centre, The Hong Kong Polytechnic University, Hung Hom, Kowloon, Hong Kong*

(Received 23 March 2010; accepted 8 December 2010; published online 11 January 2011)

Lead-free $(K_{0.48}Na_{0.48}Li_{0.04})(Nb_{0.775}Ta_{0.225})O_3$ (KNLNT) thin films were deposited on $Pt(111)/Ti/SiO_2/Si(001)$ substrates using pulsed laser deposition. The film exhibited a well-defined ferroelectric hysteresis loop with a remnant polarization $2P_r$ of 22.6 $\mu C/cm^2$ and a coercive field E_c of 10.3 kV/mm. The effective piezoelectric coefficient $d_{33,f}$ of the KNLNT thin films was found to be about 49 pm/V by piezoelectric force microscope. The dominant conduction mechanisms of Au/KNLNT/Pt thin film capacitor were determined to be bulk-limited space-charge-limited-current and Poole–Frenkle emission at low and high electric field strengths, respectively, within a measured temperature range of 130–370 K. © *2011 American Institute of Physics*. [doi:10.1063/1.3535608]

Because of the increasingly environmental concerns and legislations against the use of lead-based piezoelectric materials in the immediate future, great efforts have been made to develop high performance lead-free piezoelectric materials.[1] Among them, $(K_{1-x}Na_x)NbO_3$ (KNN hereafter) is considered to be a promising candidate owing to its pronounced ferroelectric and piezoelectric properties, high Curie temperature, and biocompatible nature. KNN thin films have been grown on various substrates by both physical and chemical approaches.[2–8] Pioneer works on thin film KNN materials were mainly focused on undoped compositions in the vicinity of morphotropic phase boundary (MPB). Good ferroelectricity and high resistivity at low electric field were reported.[8] Recent breakthrough in the textured highly piezoelectric Li, Ta, Sb doped KNN (KNN-LT-LS) ceramics by Saito *et al.*[9] has triggered intensive studies on KNN-LT-LS based thin films.[10–12] In spite of relatively high ferroelectric and piezoelectric properties, the films yet suffered from a high leakage current (e.g., $>10^{-1}$ A/cm^2 @ 10 kV/mm) and details of conduction mechanisms remain unclear. Indeed, the participation of toxic Sb in KNN-LT-LS system does not meet the ecological strategy of development of lead-free piezoelectrics.

Ours and Hollenstein's studies[13,14] have revealed that Li^+ and Ta^{5+} dual dopants can dramatically enhance the piezoelectric properties of KNN ceramics. The specific composition $(K_{0.48}Na_{0.48}Li_{0.04})(Nb_{0.775}Ta_{0.225})O_3$ (KNLNT hereafter) possesses optimal piezoelectric properties at room temperature due to the coexistence of tetragonal and orthorhombic phases. This MPB-like behavior and less processing and compositional complexity, especially the absence of toxic Sb content, as compared with KNN-LT-LS, have made KNLNT a promising candidate for biocompatible piezoelectric device applications. In this letter, we reported the excellent ferroelectric and piezoelectric properties, and low leakage current density in KNLNT thin films grown by pulsed laser deposition (PLD). Conduction mechanisms of the KNLNT thin films were investigated in detail.

The stoichiometric target of KNLNT used for laser ablation was fabricated by the conventional solid state reaction. The KNLNT thin films were deposited on $Pt(111)/Ti/SiO_2/Si(001)$ substrates by pulsed laser deposition using a KrF excimer laser (Lambda Physik COMPex 205) with a wavelength of 248 nm, a pulse width of 28 ns, and a repetition rate of 5 Hz. The laser beam impacts the rotating target with an energy density of 2 J/cm^2. The distance between the target and the substrate was fixed at 5 cm, while the substrate temperature was maintained at 680 °C. The KNLNT films of thickness ~280 nm were prepared by a number of 6000 pulses in an oxygen atmosphere of 27 Pa. After deposition, the as-grown thin films were cooled down to room temperature gradually without postannealing process. Circular Au top electrodes with diameter of 0.2 mm were prepared by rf magnetron sputtering followed by standard photolithography techniques, prior to the measurement of electrical properties.

The crystallographic characterization of the as-grown KNLNT thin films was performed on an x-ray diffractometer (Bruker AXS D8 Discover, Madison, WI). Figures 1(a) and 1(b) show the x-ray diffraction (XRD) θ-2θ scan patterns of a polycrystalline KNLNT thin film as well as a bulk KNLNT ceramic for comparison. The film exhibited a single-phase perovskite with a (110) preferred orientation. The inset of Fig. 1(a) shows the splitting of the (002)/(200) doublet of the film. The fact that (001)/(100) and (002)/(200) doublets split while (110) remains nonsplitting suggests the presence of tetragonal structure in the KNLNT film with the lattice parameters $a=3.9440$ Å and $c=3.9548$ Å. The KNLNT thin film possesses a very smooth surface with average grain size of 160–180 nm, as shown in AFM image in Fig. 1(c).

The ferroelectric hysteresis (P-E) loop was measured using a TF Analyzer 2000 equipped with a FE-Module (aixACCT). Figure 2 shows the P-E loops of the KNLNT thin

a)Authors to whom correspondence should be addressed. Electronic addresses: dy.wang@unsw.edu.au and ddmd222@yahoo.com.cn.

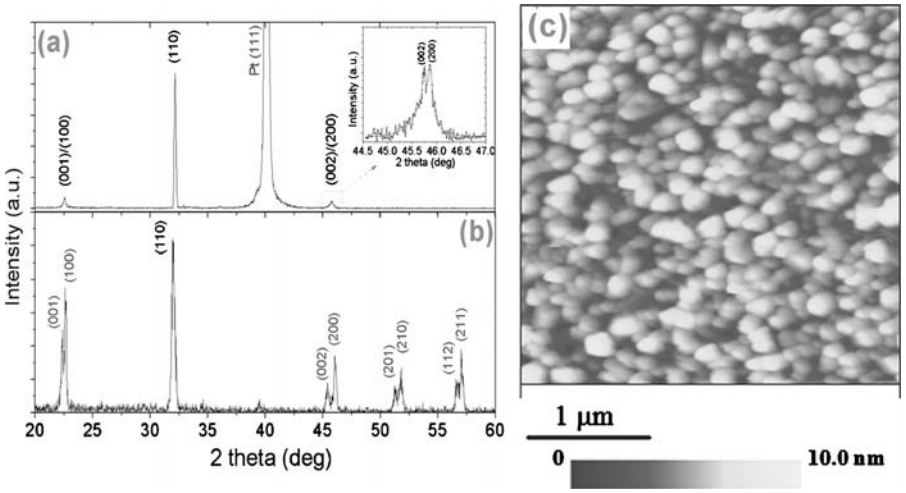

FIG. 1. (Color online) XRD θ-2θ scans of (a) KNLNT thin film grown on $Pt(111)/Ti/SiO_2/Si(001)$; (b) KNLNT bulk ceramic and (c) surface morphology of KNLNT thin film taken by AFM.

film measured under different electric fields at a frequency of 1 kHz. Well-defined *P-E* hysteresis loops are observed and the saturation of the hysteresis loop as a function of voltage is key evidence of intrinsic ferroelectricity in the KNLNT film. The observed remnant polarization $2P_r$ and coercive field E_c are 22.6 $\mu C/cm^2$ and 10.3 kV/mm, respectively. As compared to a bulk KNLNT ceramic ($2P_r = 28.8$ $\mu C/cm^2$, $E_c = 2.4$ kV/mm), the observed remnant polarization of the film is a bit lower than that of the bulks, whereas the coercive field of the film is considerably higher. This phenomenon may be attributed to the much smaller grain size of the thin film (160–180 nm versus 1–2 μm for the bulk). It has been suggested that the fine grain films with film thicknesses less than 2 μm can lead to a limited number of domain variants.[15,16] The absence of 90° domain walls and the strong pinning of non-180° domain walls lead to a decrease in P_r and an increase in E_c. Dielectric properties of Au/KNLNT/Pt capacitor were measured over a frequency range of 1–100 kHz in the temperature range of −200–200 °C using HP4284A LCR-meter. As shown in the inset of Fig. 2, both dielectric permittivity and loss tangent of KNLNT thin film increased monotonically with increasing temperature and no apparent phase transition can be observed in the measured temperature range.

Piezoresponse of the KNLNT thin film was evaluated using piezoelectric force microscope (PFM, Digital Instruments, NanoScope IV) incorporated with a standard lock-in technique. Details of the PFM measurements were presented in our previous work.[17] Figure 3 shows the variations of the static piezoresponse (amplitude) and effective $d_{33,f}$ with the bias dc electric field for a grain of the KNLNT thin film at room temperature. The amplitude of static piezoresponse exhibits a typical well-shaped "butterfly" loop, while the piezoresponse hysteresis loop is slightly distorted and offset, which might be due to the presence of nonswitchable domains pinned near then electrode-film interface.[18] Due to the different switching mechanisms between the microscopic PFM and macroscopic *P-E* measurement,[19] the observed E_c from the piezoresponse hysteresis loop is smaller than that from the *P-E* loop (8.5 kV/mm versus 10.3 kV/mm). As shown in Fig. 3, the film exhibits a maximum $d_{33,f}$ value of ~49 pm/V, which is better than PLD-produced highly *c*-axis oriented KNN ($d_{33,f}$=40 pm/V) (Ref. 20) and Mn-doped KNN-LT-LS ($d_{33,f}$=45 pm/V) (Ref. 12) thin films. The observed $d_{33,f}$ value for our KNLNT film is very comparable to those of the lead-based counterparts [$d_{33,f} = 10-110$ pm/V for typical (Pb, Zr)TiO_3 thin films[21]].

The leakage current through the Au/KNLNT/Pt capacitors was measured in a temperature range of 130–370 K using a Keithley 6517A programmable electrometer. Staircase-shaped dc bias voltage, with a 0.5 V step and 3 s span, was applied to thin film with the positive or negative potential connected to the bottom Pt electrodes. Figure 4(a) shows the typical current density *J* as a function of electric field *E* and the *J-E* characteristics were nearly symmetric with respect to voltage polarity at all temperatures. It should

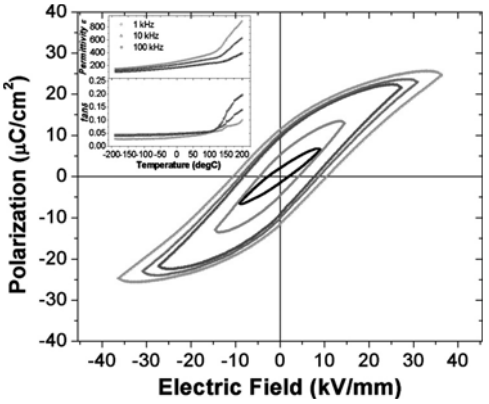

FIG. 2. (Color online) *P-E* hysteresis loops of the KNLNT thin film grown on $Pt(111)/Ti/SiO_2/Si(001)$. The inset is temperature dependence of dielectric permittivity and loss tangent of the KNLNT thin film.

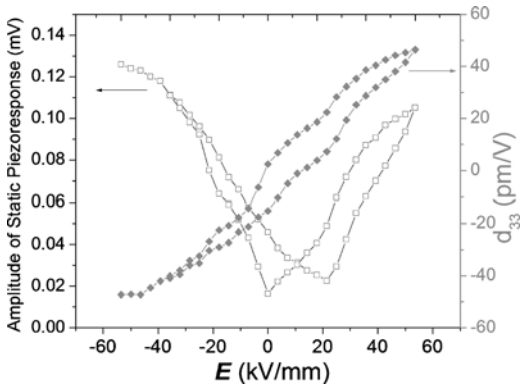

FIG. 3. (Color online) Variations of the amplitude of the static piezoresponse and the effective $d_{33,f}$ with the bias dc field for a grain of the KNLNT thin film measured at room temperature.

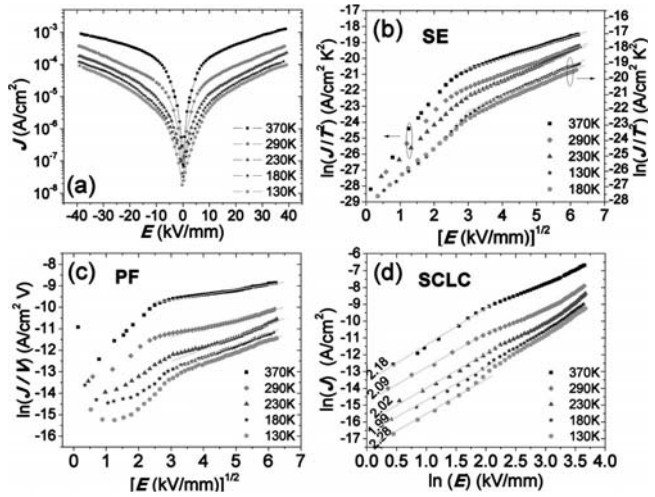

FIG. 4. (Color online) (a) Leakage current density J as a function of electric field E for the Au/KNLNT/Pt thin film capacitor at different temperatures; (b) $\ln(J/T^2)$-$E^{1/2}$ plots with respect to SE; (c) $\ln(J/V)$-$E^{1/2}$ plots with respect to PF emission; (d) $\ln(J)$-$\ln(E)$ plots with respect to SCLC.

be noted that the current density in our KNLNT thin film is remarkably lower than that in the KNN-LT-LS based films.[10–12] It is speculated that the low current density is attributed to the strong (110) orientation, as the *c*-axis oriented or columnar-grained microstructure may offer more leakage current paths through the vertically aligned grain boundaries.[16] Since no significant asymmetry in *J*-*E* behavior upon reversal of the polarity of applied voltage can be observed, we will hereafter study the situation in which Pt electrode is positively biased.

Current transport in dielectric thin films at high electric fields is usually determined to be interface-limited Schottky emission (SE) or bulk-limited Poole–Frenkel (PF) emission.[22] The current density across a Schottky barrier is[23]

$$J_S = A^* T^2 \exp - [(\phi_b - \beta_s E^{1/2})/kT], \quad (1)$$

where $\beta_s = (q^3/4\pi\varepsilon_o\varepsilon_r)^{1/2}$, A^* is the Richardson constant, T the temperature, q the electron charge, φ_b the Schottky barrier height, k the Boltzmann constant, ε_o the permittivity of free space, and ε_r the dielectric constant of the thin film. The Pool–Frenkel conductivity is given by[23]

$$J_{PF} = \sigma_0 E \cdot \exp - [(E_I - \beta_{PF} E^{1/2})/kT], \quad (2)$$

where $\beta_{PF} = (q^3/\pi\varepsilon_o\varepsilon_r)^{1/2}$, σ_0 is a sample-dependent zero-field conductivity, and E_I is the trap ionization energy. The functional relationship of SE and PF is similar so that the plots of $\ln(J/T^2)$ versus $E^{1/2}$ and $\ln(J/V)$ versus $E^{1/2}$ for SE and PF, respectively, will yield linear relationships. Figures 4(b) and 4(c) show that the data satisfy the SE and PF equations irrespective of the measuring temperature, apart from the low E field region (<10 kV/mm). Although the fittings are in good agreement with SE and PF, we are also interested in whether sensible physical parameters can be extracted from the data. The relative dielectric constants of the KNLNT film were found to be 1.7–4.1 and 5.7–14.8 for SE and PF, respectively, as calculated from the slopes of the linear fits. The physical range of ε_r for KNN-based materials is limited from one side by the optical dielectric constant $\varepsilon_\infty \approx 5$[3] and from the other side by the static dielectric constant $\varepsilon_{dc} \approx 1000$.[13] The calculated values of ε_r in SE are clearly outside this range. This demonstrates that PF emission instead of SE is the dominant conduction mechanism in our KNLNT thin films at high E field strengths.

Another possible leakage current mechanism is the bulk-limited space-charge-limited-current (SCLC), whose current density obeys quadratic electric field dependence in the case of discrete traps,[23]

$$J_{SCLC} = 9\mu\varepsilon_0\varepsilon_r E^2/8d, \quad (3)$$

where μ is the carrier mobility and d the film thickness. Figure 4(d) shows the plots of $\ln(J)$-$\ln(E)$ at different temperatures. Regardless of the measuring temperature, slopes of the linear fits were found to be around 2 at low E fields (<10 kV/mm), which is compatible with the discrete trap case of SCLC. Thus, we have clarified that leakage current behaviors of KNLNT thin film are dominated by two distinct mechanisms with respect to E field: SCLC at low E field (<10 kV/mm) and PF emission at high E field (>10 kV/mm). In addition, the *J*-*E* characteristics show little dependence on polarity of applied bias, again confirming that the leakage currents are probably bulk limited.[23]

In summary, this study investigated the ferroelectric, piezoelectric properties and leakage current behaviors of $(K_{0.48}Na_{0.48}Li_{0.04})(Nb_{0.775}Ta_{0.225})O_3$ thin films grown on $Pt(111)/Ti/SiO_2/Si(001)$ by pulsed laser deposition. The results show that the KNLNT thin film exhibits a well-defined ferroelectric hysteresis loop at room temperature with a remnant polarization $2P_r$ of 22.6 $\mu C/cm^2$ and a coercive field E_c of 10.3 kV/mm. The piezoresponse hysteresis loop was observed by PFM and the piezoelectric coefficient $d_{33,f}$ was about 49 pm/V, which is among the highest values of the reported lead-free thin films. The leakage current density in our KNLNT thin film is relatively low, which may be attributed to the strong (110) orientation. The dominant conduction mechanism in the as-grown KNLNT thin film was identified to be temperature-independent SCLC ($E<10$ kV/mm) and PF emission ($E>10$ kV/mm).

This work was supported by the Vice-Chancellor's postdoctoral fellowship program of the University of New South Wales (Grant Nos. SIR50/PS16940 and SIR30/PS20198) and the postdoctoral fellowship grant (Grant No. G-YX98) of the Hong Kong Polytechnic University.

[1]E. Cross, Nature (London) **432**, 24 (2004).
[2]C. R. Cho and A. Grishin, Appl. Phys. Lett. **75**, 268 (1999).
[3]M. Blomqvist *et al.*, Appl. Phys. Lett. **82**, 439 (2003).
[4]Y. Nakashima *et al.*, Jpn. J. Appl. Phys., Part 2 **46**, L311 (2007).
[5]P. C. Goh *et al.*, J. Am. Ceram. Soc. **92**, 1322 (2009).
[6]J. G. Wu and J. Wang, J. Appl. Phys. **106**, 066101 (2009).
[7]H. J. Lee *et al.*, Appl. Phys. Lett. **94**, 092902 (2009).
[8]S. Khartsev *et al.*, Integr. Ferroelectr. **55**, 769 (2003).
[9]Y. Saito *et al.*, Nature (London) **432**, 84 (2004).
[10]M. Abazari *et al.*, Appl. Phys. Lett. **92**, 212903 (2008).
[11]M. Abazari and A. Safari, J. Appl. Phys. **105**, 094101 (2009).
[12]M. Abazari *et al.*, J. Phys. D **43**, 025405 (2010).
[13]D. M. Lin *et al.*, J. Appl. Phys. **102**, 034102 (2007).
[14]E. Hollenstein *et al.*, Appl. Phys. Lett. **87**, 182905 (2005).
[15]D. Damjanovic, Rep. Prog. Phys. **61**, 1267 (1998).
[16]F. P. Lai *et al.*, J. Appl. Phys. **106**, 064101 (2009).
[17]D. Y. Wang *et al.*, Appl. Phys. Lett. **92**, 222909 (2008).
[18]A. L. Kholkin *et al.*, Appl. Phys. Lett. **68**, 2577 (1996).
[19]T. Watanabe *et al.*, Appl. Phys. Lett. **90**, 112914 (2007).
[20]J. S. Kim *et al.*, J. Korean Phys. Soc. **48**, 1583 (2006).
[21]P. Muralt, IEEE Trans. Ultrason. Ferroelectr. Freq. Control **47**, 903 (2000).
[22]B. Nagaraj *et al.*, Phys. Rev. B **59**, 16022 (1999).
[23]P. Zubko *et al.*, J. Appl. Phys. **100**, 114113 (2006).